



Crystal and molecular structure of calcium 1-naphthyl phosphate trihydrate
by Chi-Tang Li

A thesis submitted to the Graduate Faculty in partial fulfillment of the requirements for the degree of
DOCTOR OF PHILOSOPHY in Chemistry
Montana State University
© Copyright by Chi-Tang Li (1964)

Abstract:

The crystal and molecular structure of calcium 1-naphthyl phosphate has been solved by x-ray diffraction methods. This crystal has the following lattice parameter: $a=7.244\pm 0.002\text{\AA}$ $\alpha=84^\circ 19'\pm 3'$ $Z=2$ $b=8.994\pm 0.003\text{\AA}$ $\beta=78^\circ 32'\pm 2'$ $D_0=1.503\text{ g/ml}$ $c=18.725\pm 0.004\text{\AA}$ $\gamma=88^\circ 52'\pm 4'$ $D_c=1.508\text{ g/ml}$ Diffraction intensities were measured visually, corrected by the size factor, Lorentz and polarization factors, and the absorption factor. Intensity statistics showed that the crystal had the symmetry of $P1$.

The structure was solved with a three dimensional Patterson function, minimum function, and three dimensional Fourier synthesis. Least-squares refinements, which included first individual isotropic then anisotropic temperature factors were carried out. The final residue factor (R-factor) is 10.3% for 1724 observed reflections. The phosphate groups are distorted tetrahedrons. The four phosphate oxygens are bonded in the following manner. One oxygen is bonded to the naphthyl group, another oxygen is bonded to a hydrogen, the other two oxygens are coordinated to two calcium atoms which are related to each other by an inversion center. The neighboring phosphate groups are joined, together by hydrogen bonding between two oxygens, one of which has a hydrogen on it. Each calcium is coordinated to seven oxygens, four of which are contributed by four nearby phosphate groups, the other three from three surrounding water molecules. The calcium and the seven coordination oxygens are arranged in a distorted pentagonal bipyramid.

The pentagonal angles of O-Ca-O have the range of 67.4° to 78.6° , with the average of 72.4° (the theoretical pentagonal angle being 72°). Naphthyl groups are distorted planes. In the naphthyl groups, that side which is closest to the two nearby naphthyl groups has the shortest c-c distance of 1.30 and 1.31 \AA . The bond distances and angles are as below: P-O: 1.47 to 1.59 with the average of 1.53 \AA O-P-O angle: 103 to 117 with the average of 109 degrees C-C: 1.30 to 1.48 with the average of 1.38 \AA C-C-C angle: 116 to 125 with the average of 120 degrees The molecules are held together by strong hydrogen bonding and van der Waals forces. The successful solution of the structure has confirmed a new indexing method developed by the author. New derivations are included for each of the following formulas of equations: 1. Wolf-Bragg equation 2. Equi-inclination Weissenberg index-checking formula 3. $\sin^2 \theta$ equation for triclinic symmetry or higher 4. Triclinic interplanar spacing equation 5. Clarified forms of the x-ray Fourier synthesis equations

CRYSTAL AND MOLECULAR STRUCTURE OF CALCIUM
1-NAPHTHYL PHOSPHATE TRIHYDRATE

by

CHI-TANG LI

A thesis submitted to the Graduate Faculty in partial
fulfillment of the requirements for the degree

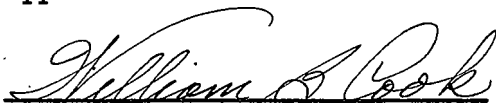
of

DOCTOR OF PHILOSOPHY

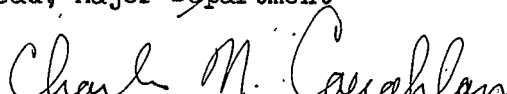
in

Chemistry

Approved:



Head, Major Department



Chairman, Examining Committee



Dean, Graduate Division

MONTANA STATE COLLEGE
Bozeman, Montana

March, 1964

ACKNOWLEDGMENT

The author wishes to express his sincere thanks to:

Dr. Charles N. Caughlan for his helpful guidance for directing this research.

National Institute of Health for the financial support.

Montana State College Computing Center for providing time on IBM 1620 electronic data processing machine.

Dr. Graeme S. Baker and Mrs. Rose L. Baker for assisting with the chemical analysis.

Mrs. Kay Roberts for reading over the dissertation and making corrections in English.

Mrs. Chi-Tang Li for immeasurable moral support and for doing the typing.

TABLE OF CONTENTS		Page
VITA		ii
ACKNOWLEDGMENT		iii
LIST OF TABLES		v
LIST OF FIGURES		viii
ABSTRACT		x
I. INTRODUCTION		1
II. EXPERIMENTAL WORK		8
III. DETERMINATION OF THE LATTICE PARAMETERS		14
IV. INDEXING TRICLINIC EQUI-INCLINATION WEISSENBERG X-RAY PHOTOGRAPH AND A METHOD OF CHECKING		25
V. UNIQUE FEATURES OF DATA REDUCTION		49
VI. STRUCTURE DETERMINATION		78
VII. REFINEMENT AND DISCUSSION OF THE STRUCTURE		116
APPENDIX		133
A. Calcium and Phosphorus Analysis		134
B. Film Processing		139
C. Weissenberg Index-Checking Results		140
D. List of Observed and Calculated Structure Factors		160
E. Derivation for the Clarified Forms of the x-ray		
Fourier Synthesis		181
LITERATURE CITED		195

Table	LIST OF TABLES	Page
I.	Chemical Analysis Results	11
II.	Determination of Cell Edge from Oscillation Data	18
III.	Determination of d_{001} from Zero Level Weissenberg Photograph	19
IV.	Determination of d_{100} from Zero Level Weissenberg Photograph	20
V.	Determination of β * Angle from Zero Level Weissenberg Photograph	21
VI.	Determination of α * Angle from Zero Level Precession Photograph	22
VII.	Possible Sets of Interaxial Angles in the Triclinic System	29
VIII.	Determination of b^* -Projection Location on $a^* c^*$ Plane.	34
IX.	Linear-Absorption Coefficient Calculation for Calcium 1-Naphthyl Phosphate	73
X.	Wilson Plot with No Correction for Calcium 1-Naphthyl Phosphate	75
XI.	Wilson Plot for Calcium 1-Naphthyl Phosphate	76
XII.	Values of F^2 for $h0l$ Reflections of Calcium 1-Naphthyl Phosphate	81
XIII.	Values of F^2 for okl Reflections of Calcium 1-Naphthyl Phosphate	83

XV.	Values of $N(z)$, in Percentages, for hol Reflections of Calcium 1-Naphthyl Phosphate	85
XIV.	Values of $N(z)$, in Percentages for okl Reflections of Calcium 1-Naphthyl Phosphate	85
XVI.	Three Dimensional Patterson Peaks Equal to or Greater than 100	96
XVII.	Patterson Peaks at Special Locations	97
XVIII.	Oxygens Found Around the First Phosphorus by Patterson Method I102
XIX.	Oxygens Found Around the Second Phosphorus by Patterson Method I102
XX.	Oxygens Found Around the First Phosphorus by Patterson Method II104
XXI.	Oxygens Found Around the Second Phosphorus by Patterson Method II104
XXII.	Carbon Positions Located by Both Minimum Function and Three Dimensional Electron Density Maps108
XXIII.	Oxygen Positions Located by Minimum Function109
XXIV.	Comparison of the Positions of All Calcium, Phosphorus, and Oxygen Atoms Located by Different Minimum Function111
XXV.	Predication of the Diffracting Power of Each Atom in Calcium 1-Naphthyl Phosphate112
XXVI.	Primary Extinction Correction for NaCl as Calculated by Lonsdale117
XXVII.	Reflections Removed Due to Primary Extinction118

XXVIII.	The Progress of Least Squares Refinement120
XXIX.	Positional Parameters of Non-Hydrogen Atoms in Fractional Coordinates and Their Estimated Standard Deviations . .	.121
XXX.	Bond Distances for Calcium 1-Naphthyl Phosphate123
XXXI.	Bond Angles for Calcium 1-Naphthyl Phosphate124
XXXII.	Comparison of Calcium 1-Naphthyl Phosphate with Other Organic Phosphates Reported130
XXXIII.	Calcium Calibration Data for Beckman Flame Quartz Spectrophotometer136
XXXIV.	Phosphorus Analysis Results by the Colorimetric Method137
XXXV.	Equi-Inclination Weissenberg Index-Checking Results for Calcium 1-Naphthyl Phosphate140
XXXVI.	List of Observed and Calculated Structure Factors160

LIST OF FIGURES

Figure	Page
1. Infra Red Chart for the Crystal Form of Calcium 1-Naphthyl Phosphate	9
2. Infra Red Chart for the Powder Form of Calcium 1-Naphthyl Phosphate	10
3. Derivation for the Oscillation Formula	15
4. Illustration of the Unique Choice of Unit Cell	28
5. An Illustration of the Indexing Procedures	33
6. Calculation of b^* -Projection on $a^* c^*$ Plane	35
7. Derivation of the Wolf-Bragg Equation	38
8. Illustration for Equi-Inclination Weissenberg Method	40
9. Orientation of Film with Respect to Camera and X-ray	45
10. Indexing Calcium 1-Naphthyl Phosphate	48
11. Scaling by the Wilson Plot Method	51
12. Reciprocal Lattice Cylindrical Coordinates for Equi-Inclination Weissenberg Photograph	54
13. The hkl Plane in Both the Rectangular and Oblique Coordinates	64
14. Computation of the Path Length for the Constant Rectangular Cross Section in the Absorption Correction	71
15. Wilson Plot for Calcium 1-Naphthyl Phosphate	77
16. Intensity Distribution for Calcium 1-Naphthyl Phosphate	86
17. okl Electron Density Projection	127
18. hko Electron Density Projection	128

19.	hol Electron Density Projection	129
20.	The Standard Calcium Calibration Curve for the Beckman Flame Quartz Spectrophotometer	135
21.	Phosphorus Calibration Curve for Beckman Model B Spectrophotometer at Wave Length 650	138
22.	Physical Meaning of the Two Dimensional Simplified Electron Density	184

ABSTRACT

The crystal and molecular structure of calcium 1-naphthyl phosphate has been solved by x-ray diffraction methods. This crystal has the following lattice parameter:

$$\begin{array}{lll} a=7.244 \pm 0.002 \text{ \AA} & b=8.994 \pm 0.003 \text{ \AA} & c=18.725 \pm 0.004 \text{ \AA} \\ \alpha=84^{\circ} 19' \pm 3' & \beta=78^{\circ} 32' \pm 2' & \gamma=88^{\circ} 52' \pm 4' \\ Z=2 & D_o=1.503 \text{ g/ml} & D_c=1.508 \text{ g/ml} \end{array}$$

Diffraction intensities were measured visually, corrected by the size factor, Lorentz and polarization factors, and the absorption factor. Intensity statistics showed that the crystal had the symmetry of $P\bar{1}$. The structure was solved with a three dimensional Patterson function, minimum function, and three dimensional Fourier synthesis. Least-squares refinements, which included first individual isotropic then anisotropic temperature factors were carried out. The final residue factor (R-factor) is 10.3% for 1724 observed reflections.

The phosphate groups are distorted tetrahedrons. The four phosphate oxygens are bonded in the following manner. One oxygen is bonded to the naphthyl group, another oxygen is bonded to a hydrogen, the other two oxygens are coordinated to two calcium atoms which are related to each other by an inversion center. The neighboring phosphate groups are joined together by hydrogen bonding between two oxygens, one of which has a hydrogen on it. Each calcium is coordinated to seven oxygens, four of which are contributed by four nearby phosphate groups, the other three from three surrounding water molecules. The calcium and the seven coordination oxygens are arranged in a distorted pentagonal bipyramid. The pentagonal angles of O-Ca-O have the range of 67.4° to 78.6° , with the average of 72.4° (the theoretical pentagonal angle being 72°). Naphthyl groups are distorted planes. In the naphthyl groups, that side which is closest to the two nearby naphthyl groups has the shortest c-c distance of 1.30 and 1.31 Å. The bond distances and angles are as below:

$$\begin{array}{l} \text{P-O: } 1.47 \text{ to } 1.59 \text{ with the average of } 1.53 \text{ \AA} \\ \text{O-P-O angle: } 103 \text{ to } 117 \text{ with the average of } 109 \text{ degrees} \\ \text{C-C: } 1.30 \text{ to } 1.48 \text{ with the average of } 1.38 \text{ \AA} \\ \text{C-C-C angle: } 116 \text{ to } 125 \text{ with the average of } 120 \text{ degrees} \end{array}$$

The molecules are held together by strong hydrogen bonding and van der Waals forces.

The successful solution of the structure has confirmed a new indexing method developed by the author. New derivations are included for each of the following formulas or equations:

1. Wolf-Bragg equation
2. Equi-inclination Weissenberg index-checking formula
3. $\sin^2 \theta$ equation for triclinic symmetry or higher
4. Triclinic interplanar spacing equation
5. Clarified forms of the x-ray Fourier synthesis equations

SECTION I

INTRODUCTION

Organic phosphates play a very important role in biological processes. The variety of the manifestations and functions of organic phosphate esters in living systems is indeed amazing. "There is hardly anything that goes on in the (living) cell in which esters of phosphoric acid, in one form or another, are not involved at some stage." (23) Two examples are cited below to illustrate the importance of organic phosphates in biological systems. (a) Deoxyribonucleic acid (DNA) which contains many organic phosphate groups, plays a key role in the storage and transport of genetic information. Crick and Watson (11) proposed an ingenious double-helix model for DNA which fits remarkably well all the facts known at the present time, and for this work, they were awarded a Nobel prize in 1962. (b) Adenosine 3',5' cyclic phosphate is a factor stimulating the conversion of inactive glycogen phosphorylase to the active form in tissue preparations. An understanding of the complicated functions of these and other organic phosphates requires basic and precise structural knowledge. The complexity of many of the substances present in living systems makes them, at least for the present, unsuitable for x-ray diffraction studies. However, a variety of simpler organic phosphates are known, and few of their structures have been determined. Although these substances may not actually be present in living systems, the basic structures should not be very much different from those in more complex molecules. Thus, solution of simpler structures will assist in present understanding as well as making solution of structures for more complex substances.

easier in the future.

Calcium 1-naphthyl phosphate was chosen for this structural study, because (a) it is very easy to obtain a good single crystal for x-ray work; (b) calcium and phosphorus atoms are fairly large suggesting use of the heavy atom method to solve the crystal structure; (c) this crystal is triclinic. Since I have worked out a method for indexing triclinic crystals as well as an index-checking method, I wanted to gain experience in using this method, even though triclinic crystals present problems not usually present in crystals of higher symmetry.

Despite the importance of knowledge of the detailed structure of organic phosphates for understanding their varied functions, relatively few structures have been accurately determined.

These few organic phosphates whose structures have been determined precisely are described briefly as below.

1. Dibenzyl phosphoric acid, $(C_6H_5CH_2)_2PO_4H$, was studied by Dunitz and Rollett (15). This crystal had the following lattice parameters:

Monoclinic with $a=20.287 \pm 0.040 \text{ \AA}$ $b=5.709 \pm 0.010 \text{ \AA}$
 $c=12.648 \pm 0.020 \text{ \AA}$ $\beta=103^\circ 13' \pm 0^\circ 10'$

$Z=4$, space group of $P2_1/a$

The final R was 11.0% for 2471 general observed reflections.

Bond distances and angles are summarized below:

For phosphate groups:

P-O (in \AA)

Range 1.469 to 1.566

-3-

Average	1.531
P-OR	1.566 & 1.545
P-OH	1.545
O-P-O (in degree)	
Range	103.8 to 117.2
Average	109.3
Angle between longest & shortest P-O	103.8 (min.)
Angle between 2 very short P-O	117.2 (max.)
P-O-C (oxygen on ester bond)	122.3 & 118.8

For benzene ring:

C-C (in Å)	
Range	1.340 to 1.407
Average	1.378
C-C-C angle (in degree)	
Range	118.5 to 121.9
Average	120.0

For close approaches between pairs of atoms indirectly covalently linked:

O-O from 2.444 to 2.573Å

O-C from 3.030 to 3.393Å

2. Calcium Thymidylate, $C_{10}H_{13}O_8N_2CaP \cdot 6H_2O$, was studied by Trueblood, Horn & Luzzati (34). This crystal had the following lattice parameters:

Monoclinic with $a=14.40 \pm 0.02\text{Å}$ $b=6.87 \pm 0.01\text{Å}$

$$c=9181 \pm 0.01 \text{ \AA} \quad \beta=90^\circ 58' \pm 3'$$

Z=2, space group of $P2_1$

The final R was 11.6% for 1575 general observed reflections.

The entire structure is held together by the Ca-O bonds and a complex network of hydrogen bonds.

For phosphate group:

P-O (in \AA)

Range 1.474 to 1.587

Average 1.515

P-OR 1.587

P-O . . . Ca 1.486 & 1.514

O-P-O (in degree)

Range 102.1 to 118.4

Average 109.3

Angle between longest & shortest P-O 102.1 (min.)

Angle between two very short P-O 118.4 (max.)

P-O-C (ester oxygen) 118.8°

C-O (PO_4) 1.472 \AA

For calcium coordination:

The environment of Ca ion is a distorted pentagonal bipyramid. Calcium coordination number is seven with four phosphate oxygens (from three different molecules) and one water molecule lying approximately in a plane and two waters on a line through the calcium nearly perpendicular to this plane.

O-O (in Å)

Range 2.29 to 2.65

Average 2.42

O-Ca-O angle (in degree)

Range 57 to 80

Average 72

3. 2-Amino-Ethanol Phosphate, $\text{NH}_3^+-\text{CH}_2-\text{CH}_2-\text{O}-\text{PO}_3\text{H}^-$, was studied by Kraut (24). This crystal had the following lattice parameters:

Monoclinic with $a=9.04^{\pm 0.02}\text{Å}$ $b=7.75^{\pm 0.02}\text{Å}$
 $c=8.86^{\pm 0.02}\text{Å}$ $\beta=102^{\circ}27'18''$

Z=4, space group of $P2_1/c$

The final R was 6.5% for 1000 observed general reflections.

Bond distances and angles for phosphate group are summarized below:

P-O (in Å)

Range 1.493 to 1.591

Average 1.536

P-OR 1.591

P-OH 1.557

Two of the oxygens on the phosphate group were reported to be attached by double bonds (1.493 & 1.503Å)

O-P-O (in degree)

Range 103.9 to 117.4

Average 109.4

Angle between longest & shortest P-O 103.9 (min.)

Angle between two very short P-O 117.4 (max.)

P-O-C (oxygen on ester bond)	118.7°
C-O (PO ₄)	1.429Å

4. Adenosine-5'-phosphate, C₁₀H₁₄O₇N₅P, was studied by Kraut &

Jensen (25). This crystal had the following lattice parameters:

Monoclinic with	a=12.77 [±] 0.92Å	b=11.82 [±] 0.02Å
	c=4.882 [±] 0.01Å	β=92°24'±5'

Z=2, space group of P2₁

The final R was 6.8% for 1197 general observed reflections.

Bond distances and angles for phosphate groups are summarized below:

P-O (in Å)

Range	1.514 to 1.610
Average	1.546
P-OR	1.610
P-OH	1.566

O-P-O (in degree)

Range	105.7 to 118.2
Average	109.4

Angle between longest & shortest P-O 105.7°(min.)

Angle between two very short P-O 118.2°(max.)

P-O-C (oxygen on ester bond) 114.7°

C-O (PO₄) 1.475Å

The following organic phosphates have been solved with either limited data or by projections. No descriptions of these structures is made here.

They are mentioned only by title.

1. "Crystal and Molecular Structure of Cytidylic Acid" by Alver &

Furberg (2)

2. "The Crystal Structure of Ba-Ribose-5-Phosphate" by Furberg & Mostad (16)

3. "The Crystal Structure of Triphenyl Phosphate" by Davies & Stanley (13)

4. "The Crystal Structure of Ba-Phenyl Phosphate" by Svetich & Caughlan (33)

SECTION II

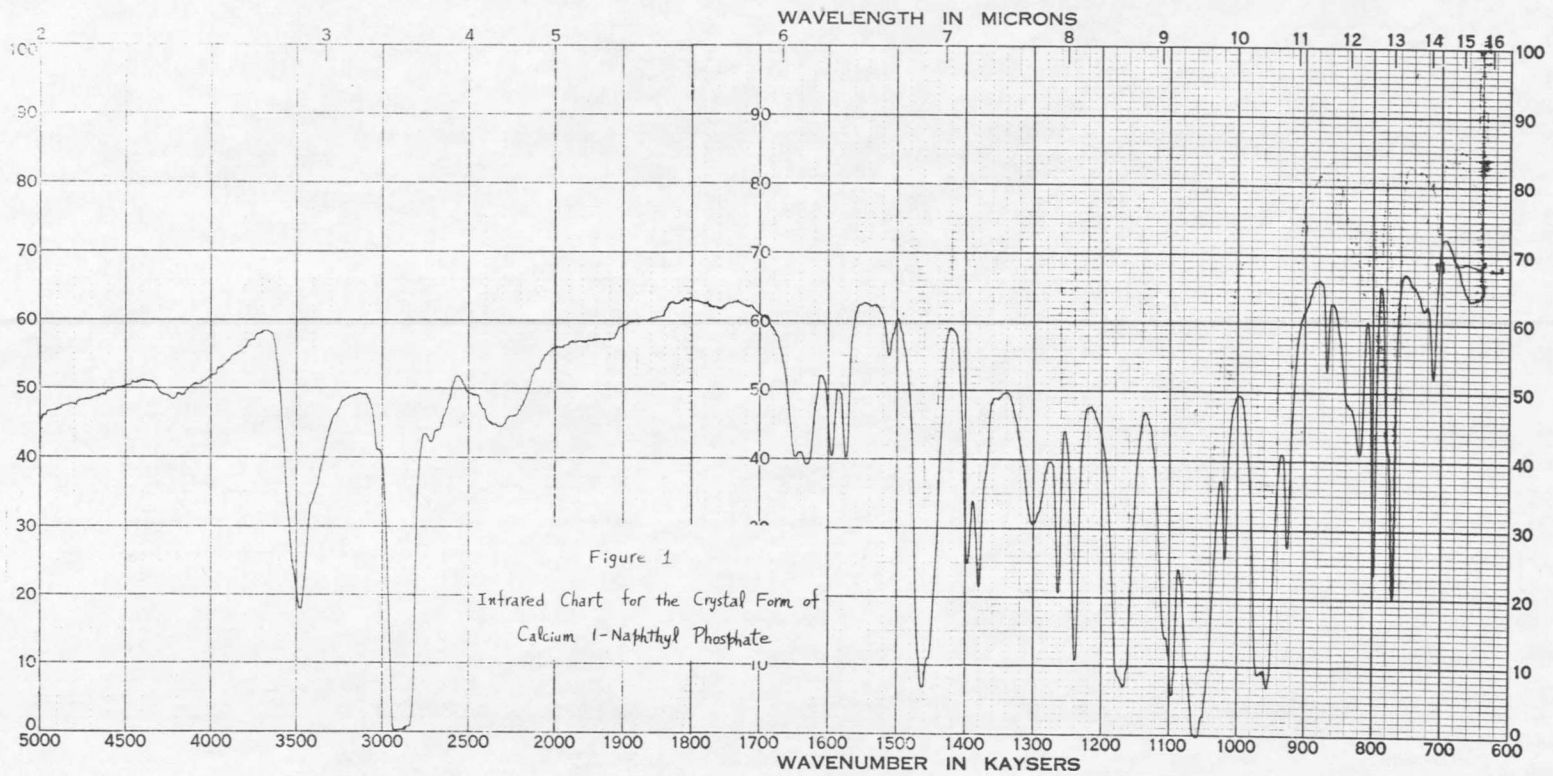
EXPERIMENTAL WORK

Preparation and identification of calcium l-naphthyl phosphate

Calcium l-naphthyl phosphate was purchased from Aldrich Chemical Company, Inc. in the form of a crystalline powder. It was purchased as $\text{Ca C}_{10}\text{H}_7\text{PO}_4 \cdot \text{H}_2\text{O}$, however chemical analysis and solution of the crystal structure have shown it to be $\text{Ca}(\text{C}_{10}\text{H}_7\text{HPO}_4)_2 \cdot 3\text{H}_2\text{O}$. To confirm the structure analysis, this compound was analyzed for calcium and phosphorus. In addition, infrared spectra were taken of the original powder and the crystals used for the structure analysis, in order to confirm that the two were identical compounds. These are shown in Fig. 1 and 2.

Calcium was determined with a Beckman Flame Quartz Spectrophotometer (Model DU) by comparing with a standard calcium solution. Phosphorus was determined by colorimetric analysis on a Beckman model B spectrophotometer by comparing with a standard phosphorus compound. Details of the analysis are included in Appendix A.

The results of the analysis, together with the comparison with the two possible structural formulas are listed in the following table. An examination of the table clearly indicates that the compound is $\text{Ca}(\text{C}_{10}\text{H}_7\text{HPO}_4)_2 \cdot 3\text{H}_2\text{O}$.



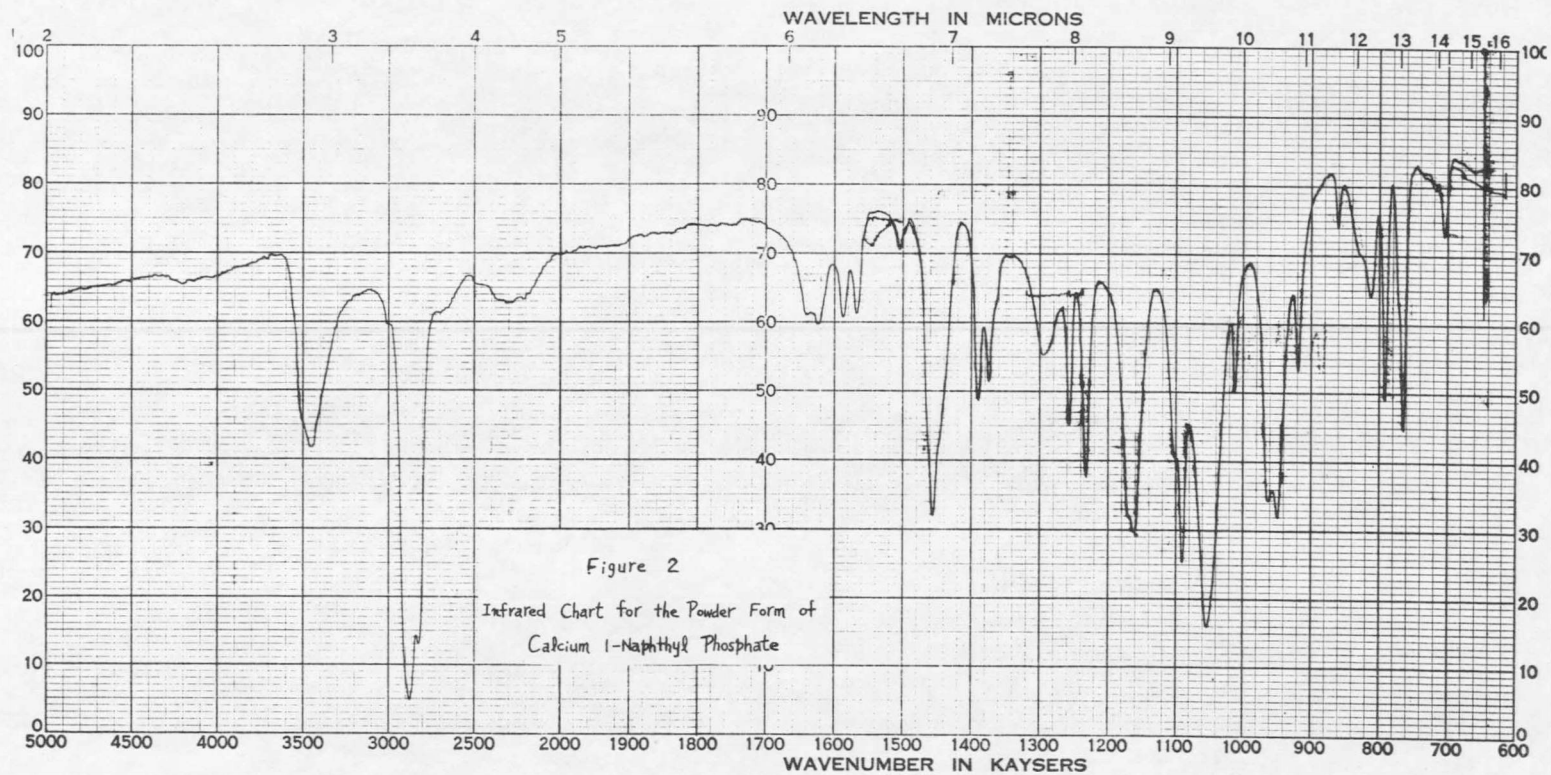


Table I. Chemical Analysis Results

Sample Analysis	$\text{Ca}(\text{C}_{10}\text{H}_7\text{HPO}_4)_2 \cdot 3\text{H}_2\text{O}$	$\text{CaC}_{10}\text{H}_7\text{PO}_4 \cdot \text{H}_2\text{O}$	
% Ca	7.916	7.416	14.320
ppm of Ca when 0.1977 gm sample diluted to 500 ml	31.3	29.3	56.6
% P	11.103	11.463	11.053
ppm of P when 0.1977 gm sample diluted to 500 ml	43.9	45.3	43.7
Atomic ratio P/Ca	1.83	2.0	1.0

Water was found to be the best solvent for obtaining good crystals, even though the solubility in water is very small. A saturated solution at room temperature was prepared, and slow evaporation at this temperature produced good single crystals. The crystal used for this x-ray work had the following approximate dimensions determined with the microscope: $1.3 \times 0.216 \times 0.125 \text{ mm}^3$.

The density was determined by the floatation method, where carbon tetrachloride diluted with ether was used as the substrate.

Test no.	Density g/ml
1	1.5027
2	1.5037

The x-ray diffraction data was obtained from Weissenberg and precession cameras, using copper radiation ($\lambda_{\text{av}} = 1.5418 \text{ \AA}$ with nickel filter). A

Phillips generator type no. 12045 B/3 series no. 57-677 and Phillips copper tube were used. Both the Weissenberg and precession cameras were Supper instruments. The Weissenberg camera (Model E of Charles Supply Company's product) has a diameter of 57.3 mm and the precession camera has a magnification factor of 60, i.e., the distance of the film to the crystal is 60 mm. Kodak medical no screen x-ray film was used. For details of film processing, see Appendix B.

Integrated photographs of three films in the camera were taken for all Weissenberg levels. Since the crystal was a triclinic, the goniometer head setting are different for precession photographs than for Weissenberg photographs. After the crystal was aligned, two integrated precession pictures (hko and okl) were taken. These pictures were used chiefly for scaling the different Weissenberg levels to a common base.

Since there are some unique features in determining the unit cell constants and indexing the photographs, these are treated in Sections 3 and 4. Intensity data were collected as described below.

Intensities of indexed photographs were obtained by visual comparison with a standard scale. The graded intensity scale was prepared in the following manner. Three film strips were put in a metal cassette in the same manner as the three films in the Weissenberg camera. The metal cassette was wrapped in a lead shield except for a small hole in the middle. The distance of metal cassette from x-ray source was 62.5 inches while the height of the small hole from ground was 49 inches. The copper x-ray tube was operated at 35 kv and 10 ma. The metal cassette was exposed to nickel-filtered copper radiation at the following time interval: 5, 10, 15, 20, 25,

30, 35, 40, 45, 50, 55, 60, 65, 70, 75, 80, 85, 90, 95, 100, 105, 110, 115, and 120 seconds. After each exposure, the film strips were moved up a few millimeters. The film strips were developed in the same manner as the integrated films and at the same time as the films for which the intensity scale is to be used. A scale was selected in the following manner and used for all the Weissenberg photographs. The darkest spot on the scale was darker than any x-ray spots on the third film (the lightest one), while the lightest spot on the scale was lighter than any spot on the third film.

Three films of the same level are called A, B, C according to the order of darkness. A is the darkest while C the lightest. Each film was read against the same scale. For many reflections there were three readings for each spot. The average ratios of A/B and A/C for each level were found. By means of these ratios, B and C films were scaled to the same level as A film. Some of the three readings were rejected for the following reason. Both ends of the scale are generally less accurate, especially the dark end due to non-linear relation between energy and optical density of film. If one such reading differed by 40% or more from the rest readings, it was rejected. Two persons were hired to read the films. Their readings on the whole were in reasonable agreement. When they were reading the same films, six readings were recorded for each spot. The average intensity for each spot was obtained by taking the average of the six readings. If the highest and lowest readings among the six differ by more than 25%, a re-check was done by the author.

SECTION III

DETERMINATION OF THE LATTICE PARAMETERS

The formulas described in this section for determining the unit cell constants are generally applicable for crystals of triclinic symmetry or higher.

This method describes use of oscillation, Weissenberg and precession photographs to obtain all the lattice parameters for a triclinic crystal. The crystal is assumed to be mounted on its b axis in the following treatment.

From oscillation photographs, the film coordinate y_n for the n^{th} level can be easily measured. If r_F is the film radius,

$$b = n\lambda(1 + (r_F/y_n)^2)^{1/2}$$

This form of the equation is derived very simply in the following way. It is shown in Fig. 3a, b, c the simple sketches of the geometrical configurations for taking the oscillation photograph. The normalized reciprocal lattice is always dimensionless. When the unit reciprocal lattice is multiplied by the film radius r_F , the sphere of reflection will fit the film exactly and the Fig. 3b is converted into Fig. 3c which is quite meaningful. In Fig. 3c, since the triangle OMP is similar to the triangle ONB, we have

$$r_F/r_F d^*_{\text{ono}} = (r_F^2 + y_n^2)^{1/2}/y_n$$

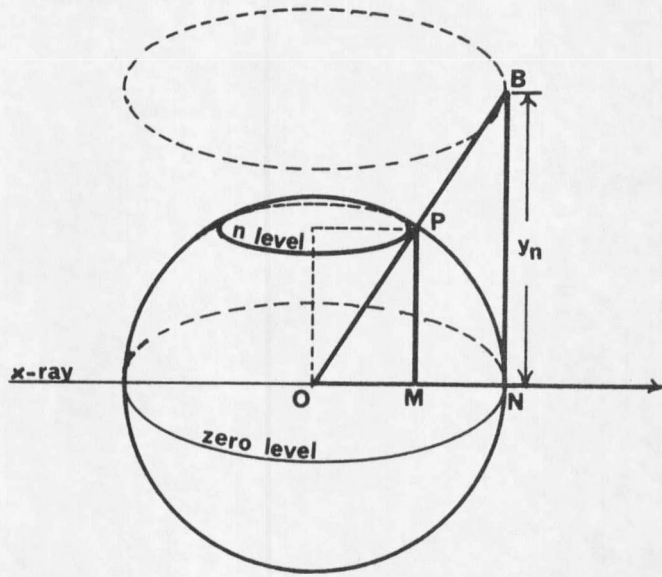
$$1/d^*_{\text{ono}} = (1 + (r_F/y_n)^2)^{1/2}$$

since $d^*_{\text{ono}} = nd^*_{\text{olo}} = n\lambda/b$

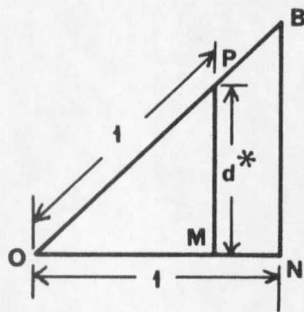
thus $b/n\lambda = (1 + (r_F/y_n)^2)^{1/2}$

or $b = n\lambda(1 + (r_F/y_n)^2)^{1/2}$

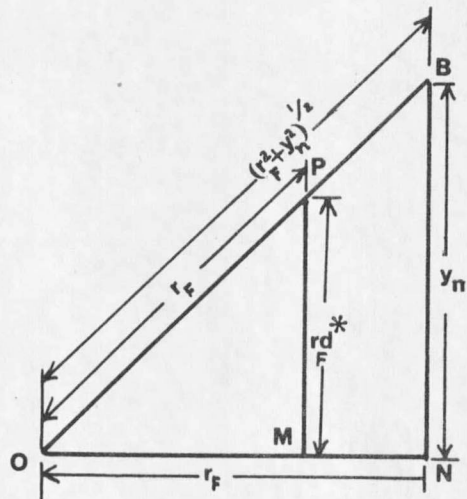
From the zero level Weissenberg photograph, the interplanar spacing of d_{100} and d_{001} and the cell edge of a and c can be found as below.



a.



b.



c.

Figure 3 Derivation for the oscillation formula

$$a = d_{100} / \sin \beta^* \sin \gamma^* = d_{100} / \sin \beta \sin \gamma^*$$

$$d_{100} = n\lambda / 2 \sin \theta_{noo}$$

For a camera of diameter 57.3 mm, $\theta_{noo} = x_{noo} / r_{noo}$ where x_{noo} is the vertical distance from the spot noo to the center line of the film.

If the film translation is 0.5 mm per degree crystal rotation

$$\beta^* = 2z / (a^* c^*)$$

where z is the horizontal distance in mm between the two axes a^* and c^* .

β^* can also be calculated by using the Wolf-Bragg equation (19). For the hol zone, the Wolf-Bragg equation takes the following form:

$$4 \sin^2 \theta_{hol} = h^2 a^{*2} + l^2 c^{*2} + 2hlc^* a^* \cos \beta^*$$

For Weissenberg camera of diameter 57.3 mm

$$\theta_{hol} = x_{hol} / r_{hol}$$

$$\cos \beta^* = (4 \sin^2 x_{hol} - h^2 a^{*2} - l^2 c^{*2}) / 2hla^* c^*$$

where $a^* = \lambda / d_{100}$

$$c^* = \lambda / d_{001}$$

Zero level precession photograph may also be used for calculation axial distances and angles.

The interplanar spacing and the cell edge are given by

$$a = d_{100} / \sin \beta^* \sin \gamma^* = d_{100} / \sin \beta \sin \gamma^*$$

$$d_{100} = n\lambda / a^*_{noo} = 60n\lambda / a^*_{noo}$$

a^*_{noo} is the actual length (in mm) measured from the point noo to the origin point on the precession picture. It is understood that the reciprocal lattice has been magnified sixty times by the precession camera (the distance from the film to the crystal is 60 mm).

The interaxial angle may be calculated either by direct measurement or

from the Wolf-Bragg equation.

(1) By direct measurement: Since the precession photograph is an undistorted picture of the reciprocal lattice, the α^* angle can be determined by the direct measurement of the angle between the axes of b^* and c^* on the b^*c^* precession photograph.

(2) By the using of Wolf-Bragg equation: For example, consider the b^*c^* precession photograph. The Wolf-Bragg equation corresponding to this has the following form.

$$\sin^2 \theta_{okl} = \frac{1}{4}(k^2 b^{*2} + l^2 c^{*2} + 2klb^*c^* \cos \alpha^*)$$

From the Bragg's law

$$\sin \theta_{okl} = (\lambda/d_{okl})/2 = \sigma_{okl}/2$$

or $\sin^2 \theta_{okl} = \sigma_{okl}^2/4$

thus $\sigma_{okl}^2 = k^2 b^{*2} + l^2 c^{*2} + 2klb^*c^* \cos \alpha^*$

$$\cos \alpha^* = (\sigma_{okl}^2 - k^2 b^{*2} - l^2 c^{*2})/2klb^*c^*$$

where σ_{okl} is the relative distance from the origin to the point okl .

Thus from the methods described above, the unit cell constants can be calculated.

The standard deviation is used here as a measure of precision. The estimated standard deviation (s. d.) per single determination is calculated by the following formula,

$$s.d. = ((d_1^2 + d_2^2 + \dots + d_n^2)/(n-1))^{1/2}$$

where d is the deviation of each single measurement from the mean, and n is the number of determinations made.

The estimated standard deviation of the mean (S. D.) is the estimated standard deviation of a single determination divided by the square of the

number of determinations.

$$S.D. = s.d. / n^{1/2}$$

1. Oscillation photograph

$$r_F = 28.45 \text{ mm (checked against NaCl)}$$

$$\lambda = 1.5418 \text{ \AA}$$

Table II. Determination of Cell Edge from Oscillation Data

n	y_n (mm)	r_F / y_n	$(r_F / y_n)^2$	$n(1 + (r_F / y_n)^2)^{1/2}$	b	%error
1	4.95	5.748	33.040	5.834	8.996	0.022
2	10.39	2.738	7.498	5.830	8.989	0.055
3	17.08	1.666	2.775	5.829	8.987	0.077
4	26.85	1.060	1.123	5.828	8.986	0.089
5	47.0	0.605	0.366	5.844	<u>9.010</u>	0.066
					Mean = 8.994 ± 0.003 \AA	

Standard deviation for a single determination = 0.007 \AA

Standard deviation of the mean = 0.003 \AA

2. Zero level Weissenberg photograph

$$\gamma = (360 / 2\pi r_F) x$$

$$r_F = 28.45 \text{ mm}$$

$$\gamma = 2.014 x$$

For zero level

$$\gamma = 2\theta$$

thus $\theta = 1.007x$

$$d_{\text{hol}} = \lambda / 2 \sin \theta_{\text{hol}} = \lambda / 2 \sin(1.007x)$$

Table III. Determination of d_{001} from Zero Level Weissenberg Photograph

ool	x_{ool} (mm)	θ_{ool}	$\sin \theta_{\text{ool}}$	d_{ool}	d_{ool}	error%
4	9.65	9.72	0.16878	4.5675	18.270	0.027
5	12.10	12.18	0.21128	3.6487	18.244	0.114
6	14.55	14.65	0.25291	3.0481	18.288	0.125
8	19.60	19.74	0.33764	2.2832	18.266	0.005
9	22.15	22.31	0.37959	2.0309	18.278	0.071
10	24.80	24.97	0.42209	1.8264	18.264	0.005
11	27.45	27.64	0.46390	1.6618	18.082	0.028
12	30.25	30.46	0.50692	1.5208	18.249	0.088
13	33.05	33.28	0.54872	1.4049	18.264	0.005
14	35.95	36.20	0.59061	1.3053	18.274	0.049
16	42.20	42.50	0.67559	1.1411	18.258	0.038
17	45.60	45.92	0.71833	1.0732	18.244	0.114
18	49.10	49.44	0.75970	1.0147	<u>18.265</u>	0.000

Mean = $18.265 \pm 0.004 \text{ \AA}$

Standard deviation for a single determination = 0.013 \AA

Standard deviation of the mean = 0.004 \AA

Table IV. Determination of d_{100} from Zero Level Weissenberg Photograph

hoo	x_{hoo} (mm)	θ_{hoo}	$\sin\theta_{hoo}$	d_{hoo}	d_{100}	error%
1	6.20	6.24	0.10870	7.0920	7.0920	0.094
2	12.45	12.54	0.21712	3.5505	7.1013	0.037
3	18.88	19.01	0.32575	2.3665	7.0995	0.011
4	25.55	25.73	0.43413	1.7757	7.1028	0.058
7	49.15	49.49	0.76041	1.0138	7.0966	0.030
8	59.88	60.30	0.86863	0.88749	<u>7.0999</u>	0.017

Mean = $7.0987 \pm 0.0017\text{\AA}$

Standard deviation for a single determination = 0.0039\AA

Standard deviation of the mean = 0.0017\AA

For β^* angle

$$\cos\beta^* = (4\sin^2\theta_{hol} - h^2 a^{*2} - l^2 c^{*2}) / 2hla^*c^*$$

$$\theta_{hol} = 1.007x_{hol}$$

$$a^* = \lambda/d_{100} = 1.5418/7.0987 = 0.21719$$

$$c^* = \lambda/d_{001} = 1.5418/18.265 = 0.084413$$

$$a^{*2} = 4.71715 \times 10^{-2}$$

$$c^{*2} = 0.71256 \times 10^{-2}$$

$$2a^*c^* = 3.66674 \times 10^{-2}$$

Table V. Determination of β^* Angle from Zero Level Weissenberg Photograph

hol	x_{hol}	e_{hol}	$\sin e_{\text{hol}}$	$4\sin^2 e_{\text{hol}}$	$\cos \beta^*$	β^*	error%
1014	35.15	35.04	0.57928	1.34226	-0.19778	101°24'	0.01
3010	28.5	28.70	0.48022	0.92244	-0.19515	101°16'	0.15
404	25.5	25.68	0.43312	0.75037	-0.20178	101°38'	0.22
5010	28.0	38.27	0.61932	1.53423	-0.19506	101°15'	0.16
708	49.9	50.25	0.76884	2.36444	-0.19626	101°19'	0.10
807	58.85	59.26	0.85949	2.95489	-0.20124	<u>101°36'</u>	0.18
Mean=101°25'±7'							

Standard deviation for a single determination=0.279°

Standard deviation of the mean =0.113°

3. Precession photograph

Since the precession camera was not calibrated with NaCl, the precision of the cell constants determined from the zero level precession photographs is uncertain. Only the α^* and γ^* angles which can not be obtained from the oscillation and zero level Weissenberg photographs are used.

γ^* angle

From the a^*b^* precession photograph, γ^* angle is found to be 90°.

α^* angle

$$\cos \alpha^* = (\sigma_{okl}^2 - k^2 b^{*2} - l^2 c^{*2}) / 2klb^*c^*$$

Table VI. Determination of α^* Angle from Zero level Precession Photograph

Distance Measured	$2 \sigma_{okl}$	σ_{okl}	$\cos \alpha^*$	α^*	error%
$0\bar{2}2-02\bar{2}$	47.0	23.5	-0.09527	$95^\circ 28'$	0.10
$0\bar{2}3-02\bar{3}$	52.8	26.4	-0.09669	$95^\circ 33'$	0.01
$0\bar{2}4-02\bar{4}$	59.75	29.88	-0.09905	$95^\circ 41'$	0.14
$0\bar{2}5-02\bar{5}$	67.4	33.7	-0.09774	$95^\circ 37'$	0.04
$0\bar{2}6-02\bar{6}$	75.55	37.78	-0.09601	$95^\circ 31'$	0.06
Mean= $95^\circ 34' \pm 5'$					

Standard deviation for a single measurement= 0.172°

Standard deviation of the mean = 0.077°

4. Calculation

The cell constants obtained from the different x-ray pictures are summarized as below.

$$b=8.994\text{\AA}$$

$$d_{100}=7.0987 \approx 7.099\text{\AA}$$

$$d_{001}=18.265\text{\AA}$$

$$\alpha^*=95^\circ 34'$$

$$\beta^*=101^\circ 25'$$

$$\gamma^*=90^\circ$$

To calculate the interaxial angles in the direct cell, we proceed as follow (6).

$$\cos \alpha = (\cos \beta \cdot \cos \gamma - \cos \alpha) / \sin \beta \cdot \sin \gamma$$

$$\alpha = 84^{\circ}19'$$

Similarly,

$$\beta = 78^{\circ}32'$$

$$\gamma = 88^{\circ}52'$$

$$a = d_{100} / \sin \gamma \cdot \sin \beta = 7.099 / 0.98004 = 7.244 \text{ \AA}$$

$$b = 8.994 \text{ \AA}$$

$$c = d_{001} / \sin \beta \sin \alpha = 18.265 / (0.98004)(0.99528) = 18.725 \text{ \AA}$$

In summary

$$a = 7.244 \pm 0.002 \text{ \AA}$$

$$b = 8.994 \pm 0.003 \text{ \AA}$$

$$c = 18.725 \pm 0.004 \text{ \AA}$$

$$\alpha = 84^{\circ}19' \pm 3'$$

$$\beta = 78^{\circ}32' \pm 2'$$

$$\gamma = 88^{\circ}52' \pm 4'$$

Let V be the unit cell volume

$$V = abc \sin \alpha \sin \beta \sin \gamma$$

$$= (7.244)(8.994)(18.725)(0.99508)(0.98004)$$

$$= (65.153)(18.261)$$

$$= 1,189.8 \text{ \AA}^3$$

For $\text{Ca}(\text{C}_{10}\text{H}_7\text{HPO}_4)_2 \cdot 3\text{H}_2\text{O}$

$$\text{Molecular weight} = 540.426$$

$$\text{Density} = 1.5031 \text{ g/ml}$$

$$\text{Molecular volume} = 540.426 / (1.5031)(0.6023)$$

$$= 540.426 / 0.90531$$

$$= 596.9 \text{ \AA}^3$$

$$\text{Number of molecules per unit cell} = 1,189.8 / 596.9$$

$$= 1.993$$

Let D_o and D_c be observed and calculated density respectively.

-24-

$$D_o = 1.503 \text{ g/ml}$$

$$D_c = 1.503 (2/1.993)$$

$$= 1.508 \text{ g/ml}$$

SECTION IV

INDEXING THE TRICLINIC EQUI-INCLINATION

WEISSENBERG X-RAY PHOTOGRAPH AND A METHOD OF CHECKING

Usually, x-ray diffraction photographs taken by the equi-inclination Weissenberg method can be indexed routinely. However, for triclinic crystals, certain problems arise in the indexing and it is worth while examining the methods used here.

It is not difficult to index the zero level triclinic Weissenberg photograph. Problems start when we try to index the upper level triclinic equi-inclination Weissenberg pictures. This is because the reciprocal lattice axial lines of a triclinic crystals do not show up as straight lines on the upper equi-inclination Weissenberg photographs. The method outlined here offers not only the correct indexing but also the unique choice of unit cell.

For the triclinic system, since there is no symmetry except possibly an inversion center, a primitive cell is always chosen. There are many ways to choose a primitive cell in a triclinic lattice. Given the three translations of the primitive cell edges x , y , z and the three axial labels a , b , and c , there are six ways of fixing a , i.e., x , $-x$, y , $-y$, z , and $-z$. If a is assigned as x or $-x$, there are four ways to fix b , that is y , $-y$, z and $-z$. Then, if a right hand coordinate system is chosen, c is automatically fixed. Thus, there are a total of twenty-four possible ways of fixing labels to the translations. Balashov (3,4) devised some rules, which will theoretically lead to a unique choice.

Balashov's method:

1. Select a primitive cell having the smallest volume.
2. Let $c > b > a$

This rule follows Buerger's convention (6). Usually, this will lead to $a^* > b^* > c^*$. Donnay and Nowacki (14) suggested a different order-convention; $b > a > c$. The reason they prefer c as the shortest axis is that crystals ordinarily grow so that they are elongated parallel to the shortest translations and the choice of c for the shortest translation causes the crystal to look like a vertical column. On the other hand, the Buerger's convention $c > b > a$ has the following advantages as indicated by Balashov (2); (a) It is convenient for tabulation purposes (b) It can be used for tetragonal and hexagonal crystals, where (in contrast to the orthorhombic system) the c and a axes are fixed by symmetry convention, the ratio c/a is greater than unity, i.e., c is greater than a which violated Donnay's convention.

3. Let α, β, γ be homogeneous, that is, all obtuse or all acute.

The ordinary procedure of doing this is first to choose $\alpha^*, \beta^*, \gamma^*$ all acute. If α, β, γ do not turn out all obtuse, adjust α^*, β^* , or γ^* (by taking their supplement) until α, β, γ are all acute. Some people prefer that all α, β, γ be non-acute. To convert all acute angles to all obtuse ones, the Delaunay Reduction (20) may be used. The Delaunay Reduction gives the cell which has the three interaxial angles (α, β, γ) all non-acute, and within the limits imposed by this condition, the three translations a, b, c the shortest possible. The Delaunay Reduction is based on the following principles: the reciprocal of an

obtuse parallelepiped is an acute one and usually vice versa.

To show that the Balashov's method leads to an unique choice of unit cell, proceed as follows.

Fig. 4 a, b shows the general arrangement of three axial labels a, b, c and the interaxial angles α, β, γ , as well as the projection of c axis on ab plane.

If the projection of c-axis or z lies in the MxN zone, i.e., on the positive x side of the perpendicular to x as shaded, angle xoz or β is acute.

Similarly, if the projection of z lies in the TyS zone, i.e., on the positive y side of the perpendicular to y as shaded, angle yoz or α is acute.

Since xyz_1 rotated 180 degree equal to $\bar{x}\bar{y}z_3$

xyz_2 rotated 180 degree equal to $\bar{x}\bar{y}z_4$

there are only two kinds of triclinic crystals, i.e., axial system like xyz_1 (type 1) and xyz_2 (type 2).

Type 1: xyz_1

α or yoz is acute

β or xoz is acute

γ or xoy is acute

Type 2: xyz_2

α or yoz is acute

β or xoz is obtuse

γ or xoy is acute

We can have different representations of the triclinic crystal

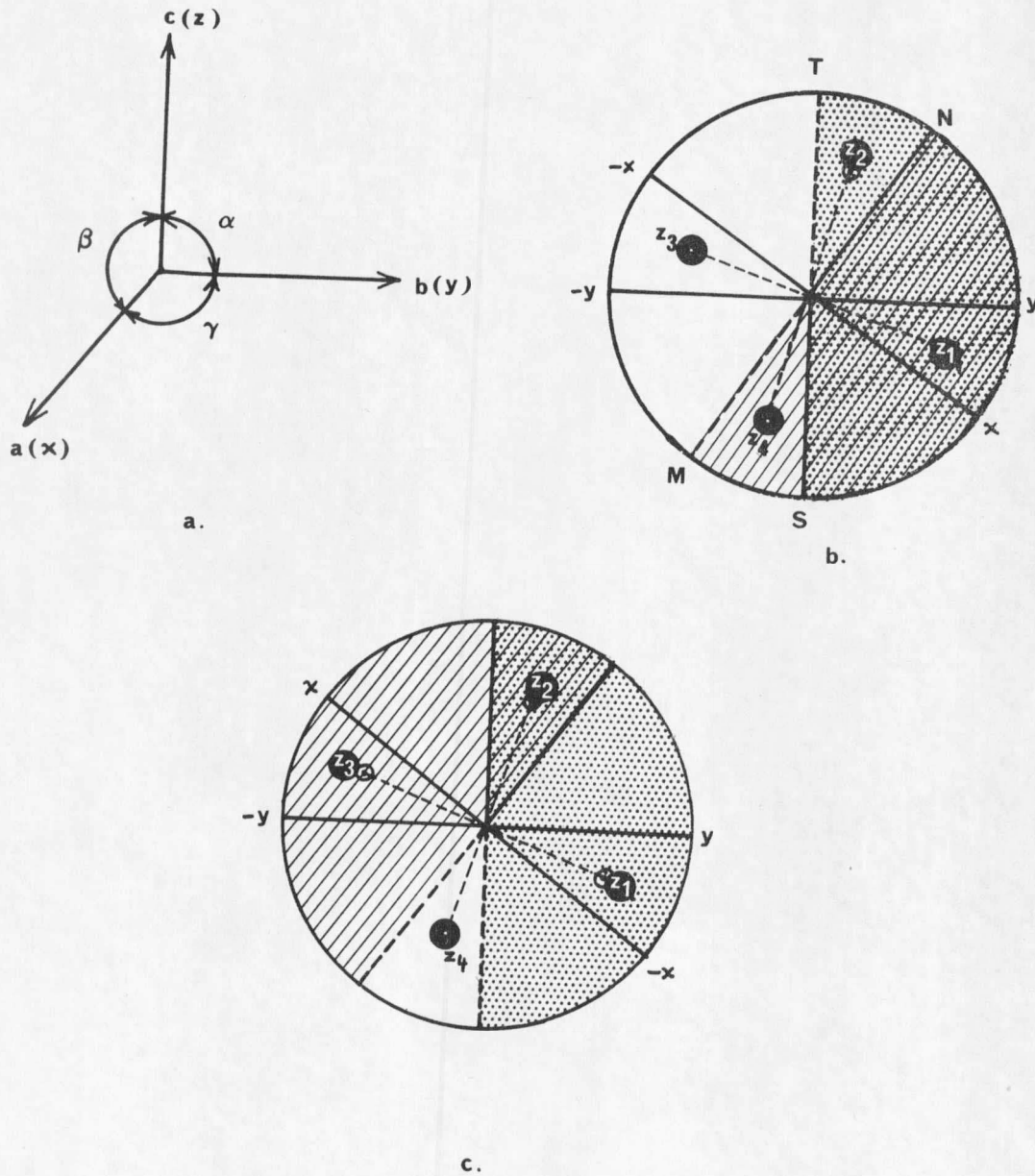


Figure 4 Illustration of the unique choice for the unit cell

by different combinations of acute and obtuse angles.

For example, if a is changed from plus x to minus x , the character of β and γ changes from acute to obtuse or vice versa, as shown in Fig. 4 c.

Type 1: $\bar{x}yz_1$

α or yoz is acute

β or xoz is obtuse

γ or xoy is obtuse

Type 2: $\bar{x}yz_2$

α or yoz is acute

β or xoz is acute

γ or xoy is obtuse

Following the same procedure, we can have all the possible arrangements of a , b , c and the angle characters as listed in the following table. (table in Buerger (7) with corrections)

Table VII. Possible Sets of Interaxial Angles in the Triclinic System

Type 1 crystal

Orientation	cos	Type of Coordinate System	Designation of Representation	
abc is xyz_1	+ + +	R	1R	Normal
abc is $\bar{x}yz_1$	+ - -	L	3L	
abc is $\bar{\bar{x}}yz_1$	- - +	R	2R	
abc is $x\bar{y}z_1$	- + -	L	4L	
abc is $\bar{\bar{x}}\bar{\bar{y}}z_1$	+ + +	L	1L	Normal
abc is $x\bar{\bar{y}}z_1$	+ - -	R	3R	
abc is $xy\bar{\bar{z}}_1$	- - +	L	2L	

Orientation	cos	Type of Coordinate System	Designation of Representation
abc is $\bar{x}\bar{y}\bar{z}_1$	- + -	R	4R
<u>Type 2 Crystal</u>			
abc is xyz_2	+ - +	R	1R
abc is $\bar{x}yz_2$	+ + -	L	3L
abc is $\bar{x}\bar{y}z_2$	- + +	R	2R
abc is $\bar{x}yz_2$	- - -	L	4L Normal
abc is $\bar{x}\bar{y}\bar{z}_2$	+ - +	L	1L
abc is $xy\bar{z}_2$	+ + -	R	3R
abc is $xy\bar{z}_2$	- + +	L	2L
abc is $\bar{x}y\bar{z}_2$	- - -	R	4R Normal

A crystal can be either one of the two crystal types and can not be both at the same time. Hence, once the type of coordinate system is chosen, there is only one case for the interaxial angles to be all acute or all obtuse. Balashov's method of letting α, β, γ be all obtuse or all acute is thus justified.

A suggested indexing method for the triclinic Weissenberg photographs:

In the equi-inclination Weissenberg method, the camera is so inclined that the direct x-ray beam and the diffracted beam are equally inclined to the layers of the reciprocal lattice. The equi-inclination keeps the reciprocal lattice rotation axis exactly on the circumference of the reflecting circle of the n-layer.

Certain indexing problems arise for triclinic crystals for which Weissenberg photographs are taken. It should be understood that x-ray

diffraction photographs provide a picture of the reciprocal lattice. For the ease of illustration, it is assumed that the crystal is mounted on b axis unless otherwise specified. The two reciprocal axes a^* and c^* will show up as straight lines on the zero Weissenberg photograph and the photograph is indexed in the normal manner. In indexing the upper level Weissenberg photographs for triclinic crystal, the reciprocal lines $h10$, $h20$, $01l$, $02l$ etc. no longer appear as straight lines. If any reciprocal lattice axial line e.g. hno , or onl passes through the rotation axis, a straight line will result on all the equi-inclination Weissenberg levels. This can occur if any upper level reciprocal lattice line projection on the zero level coincides with the a^* or c^* . For orthogonal systems this is always the case, for monoclinic systems it is the case if the crystal is mounted on b , but not so if mounted on a or c , and would only be accidentally the case for triclinic crystals. However, for any non-orthogonal crystal, a non-axial reciprocal lattice line may, on one level or another, accidentally pass through the rotation center, producing a straight line on the equi-inclination Weissenberg photograph. Thus, for triclinic crystal, usually no upper level reciprocal lattice line will pass through the rotation axis. The problem of indexing the triclinic upper level equi-inclination Weissenberg photographs is to recognize the reciprocal lattice lines. Assuming all the reciprocal lattice lines on the zero level are known, the easy way to do this is to project the upper levels onto the zero level. Fig. 5 a represents the zero level where the point O is the rotation center, the horizontal line passing through the rotation center is the c^* axis

or o_0l line, and the line passing through the point O and making an angle β^* with c^* is a^* axis or h_0o line. All the upper level reciprocal lattice points o_k must lie on the b^* axis. The length and positions of the b^* axis projection on the zero level $a^* c^*$ plane can be calculated (For calculation, see next paragraph). The positions of the point o_k corresponding to the k^{th} level can thus be located. From o_k , construct the k^{th} level reciprocal lattice network hkl by drawing lines parallel to a^* and c^* . Consider the four reciprocal lattice lines sitting closest to the rotation center, O . These represent the four festoons next to the two straight axial lines of the zero level projected onto the k^{th} level. The festoon at the right or left of a^* projection corresponds to the right or left reciprocal lattice lines of a^* in Fig. 5 a. The other two festoons can be identified in the same manner. Once these four festoon (the reciprocal lattice lines) have been indexed properly, there is no problem indexing the other reciprocal lattice points. An illustration of these procedures is shown in Fig. 5.

A calculation for the length and location of the axial projection:

First obtain all the reciprocal lattice cell constants a^* , b^* , c^* and α^* , β^* , γ^* . From these, the reciprocal lattice unit cell is constructed as shown in Fig. 6 where three axes meet at the point O , and OA , OB , OC represent the unit length of a^* , b^* and c^* respectively. Then, in the BOC plane ($b^* c^*$ plane), draw BN perpendicular to OC . From B , draw line BM perpendicular to the plane AOC ($a^* c^*$ plane). Connect NM and OM . From the geometrical relation, we have

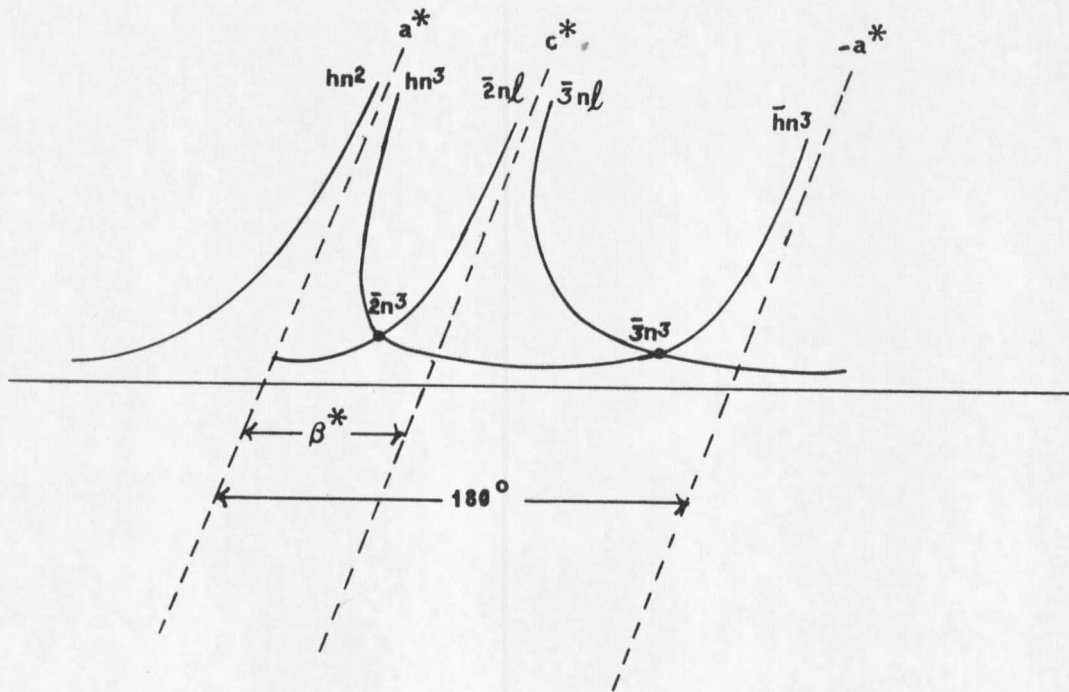
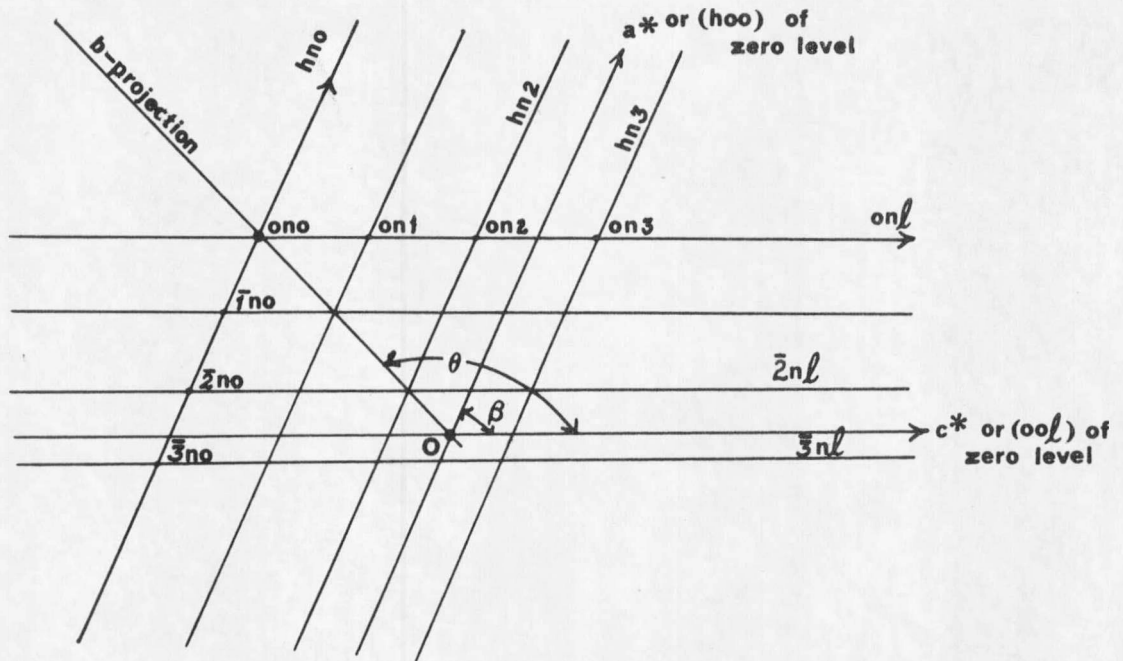


Figure 5 An illustration of the indexing procedures

$$ON = b \cdot \cos \alpha$$

$$BN = b \cdot \sin \alpha$$

Angle BNM = $180 - \gamma$ (for derivation, see Buerger (6))

$$BM = b \cdot \sin \alpha \cdot \sin \gamma$$

$$NM = -b \cdot \sin \alpha \cdot \cos \gamma$$

$$OM = b \cdot (1 - \sin^2 \alpha \cdot \sin^2 \gamma)^{1/2}$$

$$\cos p = (ON^2 + OM^2 - MN^2) / 2ON \cdot OM$$

$$= ((b \cdot \cos \alpha)^2 + b^2 (1 - \sin^2 \alpha \cdot \sin^2 \gamma) - (b \cdot \sin \alpha \cdot \cos \gamma)^2) / 2(b \cdot \cos \alpha) b (1 - \sin^2 \alpha \cdot \sin^2 \gamma)^{1/2}$$

Where OM is the unit length of b^* projection on $a^* c^*$ plane.

p is the location of b^* projection on $a^* c^*$ plane (the angle between b^* projection and c^*).

It is noted that the approximate location of b^* projections can be determined as follows by the interaxial angles α^* and γ^* only.

Table VIII. Determination of b^* - Projection Location on $a^* c^*$ Plane.

Interaxial angles		Quadrant where b^* projection lies
acute	acute	1
obtuse	obtuse	3
acute	obtuse	4
obtuse	acute	2

Index-checking method:

The index-checking method will serve as a check on proper

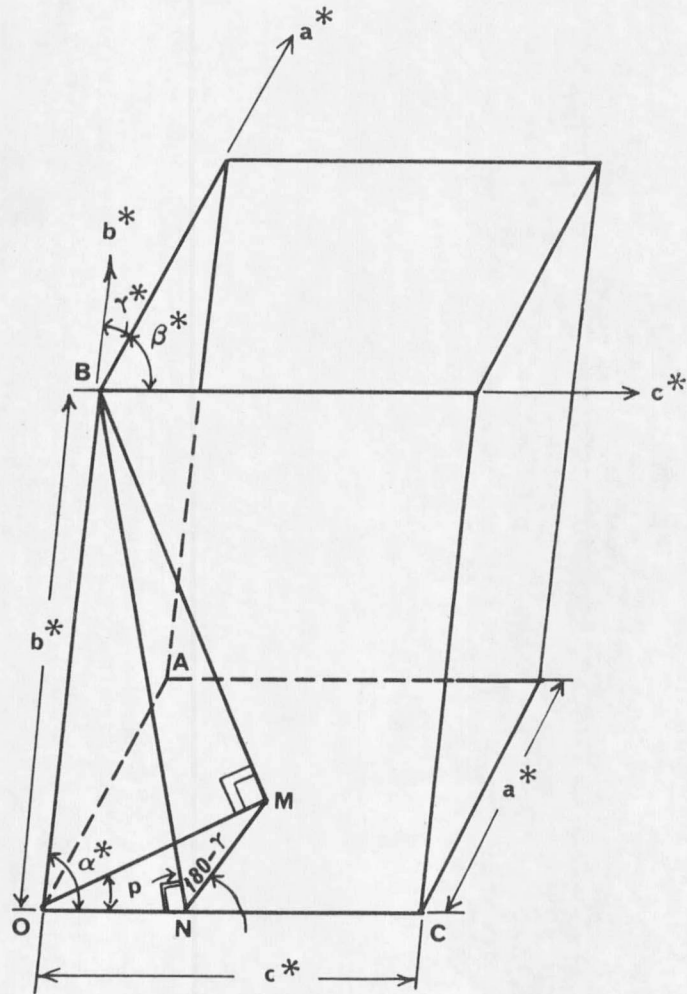


Figure 6 The calculation of b^* -projection on a^*c^* plane

indexing of the equi-inclination Weissenberg photographs. The calculation of the vertical distance of the hkl reflection from the equator line; $x_{\text{calc.}}$ is compared with the measured distances $x_{\text{obs.}}$. If the percentage error (error%)

$$\text{Error \%} = (x_{\text{obs.}} - x_{\text{calc.}}) / x_{\text{obs.}}$$

equal or less than 5%, a correct indexing is assumed.

Index-checking formulas:

For equi-inclination Weissenberg method

$$x_{\text{calc.}} = \frac{1}{2} \cos^{-1} (2(1 - \sin^2 \theta) / \cos^2 \mu - 1)$$

Where μ is the angle of inclination

$\sin^2 \theta$ may be calculated from Wolf-Bragg equation as below:

$$4 \sin^2 \theta_{\text{hkl}} = h^2 a^{*2} + k^2 b^{*2} + l^2 c^{*2} + 2hka^*b^* \cos \gamma^* + 2klb^*c^* \cos \alpha^* + 2lhc^*a^* \cos \beta^*$$

Derivation of index-checking formulas:

a. Wolf-Bragg equation

Note: The Wolf-Bragg equation is not present in many standard reference books. I found this equation in a Russian journal (19,5), translated and sent to me by V. Balashov. Since I could not find a derivation for this equation in the literature, a derivation is included here.

A reciprocal lattice vector \vec{G}_{hkl} is a vector, drawn from the reciprocal lattice origin to the reciprocal lattice point hkl as shown in Fig. 7 a. It has three components ha^* , kb^* , and lc^* along the three axial directions.

From the vector analysis, we have

$$\begin{aligned}\vec{\sigma}_{hkl} &= h\vec{a}^* + k\vec{b}^* + l\vec{c}^* \\ \sigma_{hkl}^2 &= \vec{\sigma}_{hkl} \cdot \vec{\sigma}_{hkl} \\ &= (h\vec{a}^* + k\vec{b}^* + l\vec{c}^*) \cdot (h\vec{a}^* + k\vec{b}^* + l\vec{c}^*) \\ &= h^2 a^{*2} + k^2 b^{*2} + l^2 c^{*2} + 2hka^* \cdot b^* + 2klb^* \cdot c^* + 2hla^* \cdot c^*\end{aligned}$$

Since $\vec{a}^* \cdot \vec{b}^* = a^* b^* \cos \gamma^*$, $\vec{b}^* \cdot \vec{c}^* = b^* c^* \cos \alpha^*$,

$$\vec{a}^* \cdot \vec{c}^* = a^* c^* \cos \beta^*$$

$$\begin{aligned}\sigma_{hkl}^2 &= h^2 a^{*2} + k^2 b^{*2} + l^2 c^{*2} + 2hka^* b^* \cos \gamma^* + 2klb^* c^* \cos \alpha^* \\ &\quad + 2hla^* c^* \cos \beta^*\end{aligned}$$

From Bragg's equation (Fig. 7b)

$$\lambda = 2d_{hkl} \sin \theta_{hkl}$$

or $4 \sin^2 \theta_{hkl} = (\lambda/d_{hkl})^2 = \sigma_{hkl}^2$

Combining the above equations, we have

$$\begin{aligned}4 \sin^2 \theta_{hkl} &= h^2 a^{*2} + k^2 b^{*2} + l^2 c^{*2} + 2hka^* c^* \cos \gamma^* \\ &\quad + 2klb^* c^* \cos \alpha^* + 2hla^* c^* \cos \beta^*\end{aligned}$$

b. Equi-inclination Weissenberg index-checking formula

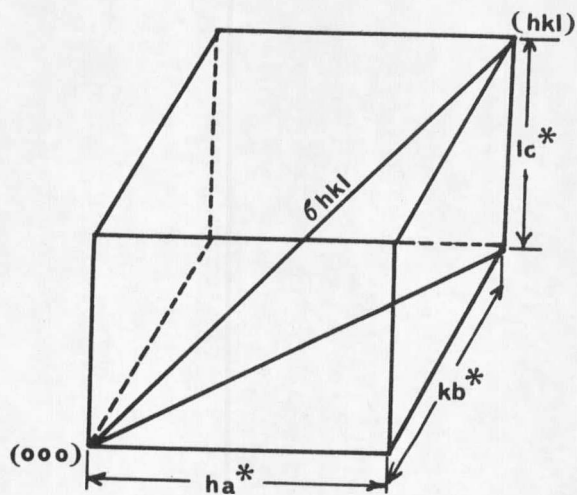
Fig. 8 a, b illustrates the equi-inclination method in three dimensions and the important part of the spherical surface diagram. The crystal is sitting at the center of a unit radius sphere (sphere of reflection). Since the angle (in radian) subtended from the center of a sphere or a circle is equal to the arc length divided by the radius and the radius of the sphere of reflection is unit,

$$\widehat{PO} = 2\theta$$

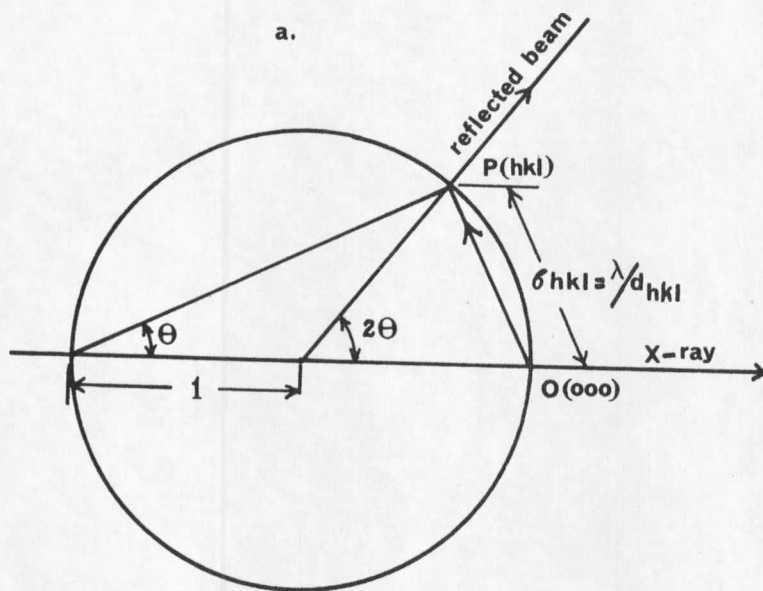
$$\widehat{AB} = \gamma$$

$$\widehat{PA} = \chi$$

$$\widehat{BO} = \mu$$



a.



b.

Figure 7 Derivation of the Wolf-Bragg equation

Where θ is the Bragg glancing angle

$\chi = \tan^{-1} y_n / r_F$, y_n is the distance from n^{th} level line to the center line in an oscillation picture, r_F is the film radius.

γ is the general reflection angle

μ is the inclination angle

Note that

Angle PAB=90 degree, Angle ABO=90 degree

Angle PAO=90 degree + Angle BAO

From the spherical geometry, the following equations are true:

(1) For right spherical triangle

$$\cos c = \cos a \cos b, \quad \sin A = \sin a / \sin c$$

(2) For oblique spherical triangle

$$\cos a = \cos b \cos c + \sin b \sin c \cos A$$

Let $\widehat{AO} = y$, Angle BAO = z

Since ABO is a right spherical triangle (Angle ABO is 90 degree),

$$\cos y = \cos \mu \cos \gamma \dots \dots \dots (1)$$

or $\sin y = (1 - \cos^2 \mu \cos^2 \gamma)^{1/2}$

$$\begin{aligned} \sin z &= \sin \mu / \sin y \\ &= \sin \mu / (1 - \cos^2 \mu \cos^2 \gamma)^{1/2} \dots \dots \dots (2) \end{aligned}$$

PAO is an oblique spherical triangle; thus

$$\begin{aligned} \cos 2\theta &= \cos \chi \cos y + \sin \chi \sin y \cos(90+z) \\ &= \cos \chi \cos y - \sin \chi \sin y \sin z \dots \dots \dots (3) \end{aligned}$$

Substituting equations (1) and (2) into equation (3),

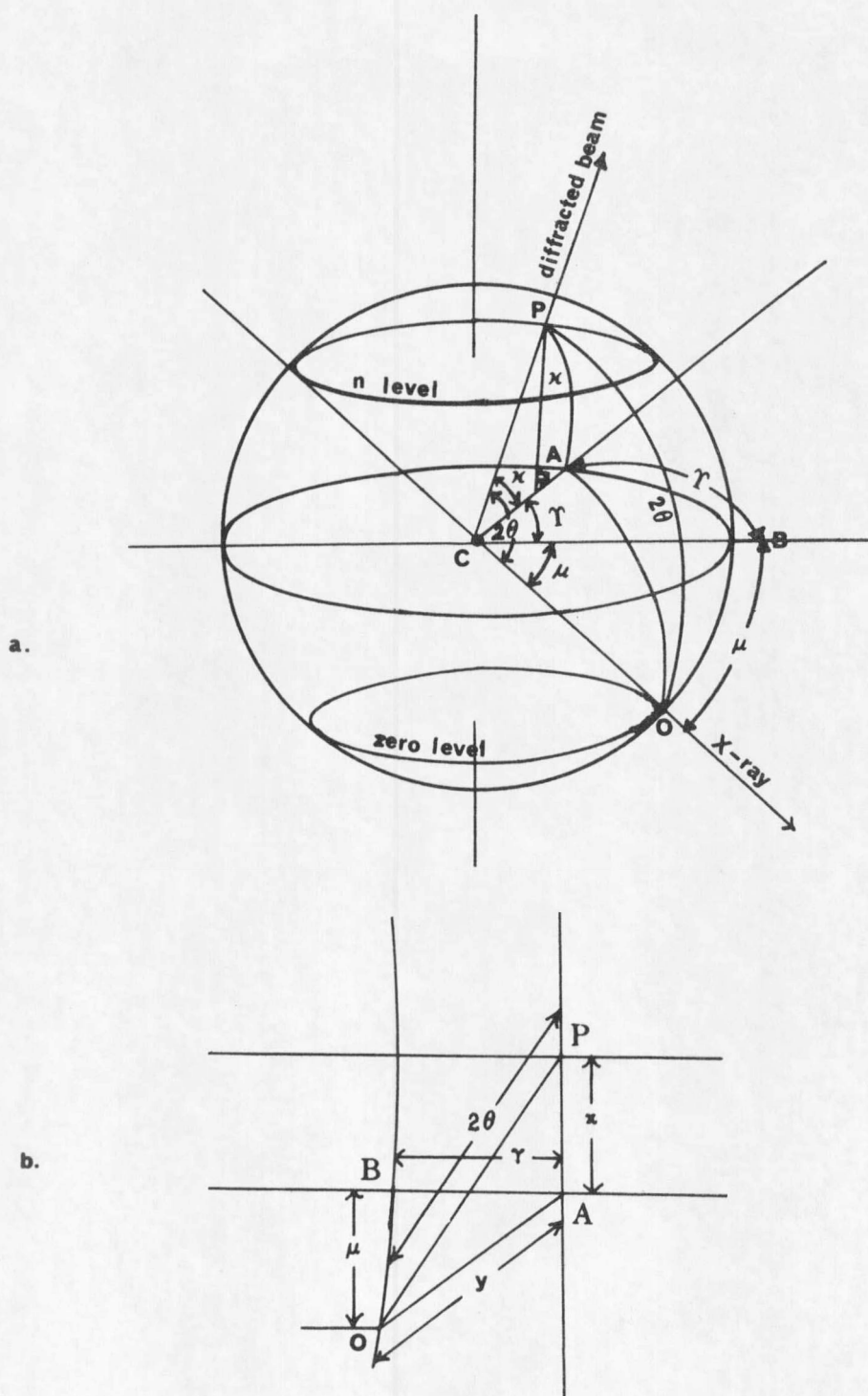


Figure 8 a. Illustration for equi-inclination Weissenberg method
b. The important spherical surface diagram

$$\begin{aligned} \cos 2\theta &= \cos \chi \cos \mu \cos \gamma - \sin \chi \sin \mu / \sin \gamma \\ &= \cos \chi \cos \mu \cos \gamma - \sin \chi \sin \mu \end{aligned}$$

For equi-inclination method

$$\chi = \mu$$

$$\begin{aligned} \text{Thus, } \cos 2\theta &= \cos^2 \mu \cos \gamma - \sin^2 \mu = \cos^2 \mu \cos \gamma - 1 + \cos^2 \mu \\ &= \cos^2 \mu (1 + \cos \gamma) - 1 \dots \dots \dots (4) \end{aligned}$$

$$\begin{aligned} \text{or } \cos \gamma &= \frac{1 + \cos 2\theta}{\cos^2 \mu} - 1 \\ &= \frac{1 + 1 - 2\sin^2 \theta}{\cos^2 \mu} - 1 \\ &= \frac{2(1 - \sin^2 \theta)}{\cos^2 \mu} - 1 \end{aligned}$$

$$\text{Therefore, } \gamma = \cos^{-1} \left[\frac{2(1 - \sin^2 \theta)}{\cos^2 \mu} - 1 \right]$$

D. Application

The unique choice of unit cell and the indexing methods for the triclinic crystals are applied to the triclinic crystal of calcium l-naphthyl phosphate $\text{Ca}(\text{C}_{10}\text{H}_7\text{HPO}_4)_2 \cdot 3\text{H}_2\text{O}$. The results which will, in turn, serve as an illustration of the above methods will be reported in the following sections.

1. Unique choice of unit cell for calcium l-naphthyl phosphate.

A direct calculation from the oscillation, zero level Weissenberg, and precession photographs gives us the following cell constants.

$$\begin{aligned} d_{100} &= 7.099 \text{ \AA} \\ b &= 8.994 \text{ \AA} \end{aligned}$$

$$d_{001} = 18.265 \text{ \AA}$$

$$\alpha^* = 95^\circ 34' \text{ or } 84^\circ 26'$$

$$\beta^* = 101^\circ 25' \text{ or } 78^\circ 35'$$

$$\gamma^* = 90^\circ$$

Since d_{100} and d_{001} are not too far from a and c respectively, the Balashov's second rule i.e., $c > b > a$ is temporarily used to assign the above labels.

To see whether all angles α , β , γ are homogeneous, first take α^* , β^* , γ^* all acute.

$$\alpha^* = 84^\circ 26'$$

$$\beta^* = 78^\circ 35'$$

$$\gamma^* = 90^\circ$$

$$\text{Then, } \sin \alpha^* = 0.99528$$

$$\cos \alpha^* = 0.09700$$

$$\sin \beta^* = 0.98021$$

$$\cos \beta^* = 0.19794$$

$$\sin \gamma^* = 1.0$$

$$\cos \gamma^* = 0.0$$

$$\text{Thus, } \cos \alpha = \frac{\cos \beta^* \cos \gamma^* - \cos \alpha^*}{\sin \beta^* \sin \gamma^*}$$

$$\cos \alpha = (0 - 0.09700) / 0.98021 = -0.09896$$

$$\alpha = 95^\circ 41'$$

$$\cos \beta = (\cos \alpha^* \cos \gamma^* - \cos \beta^*) / \sin \alpha^* \sin \gamma^*$$

$$= -0.19794 / 0.99528 = -0.19888$$

$$\beta = 101^\circ 28'$$

$$\cos \gamma = (\cos \alpha^* \cos \beta^* - \cos \gamma^*) / \sin \alpha^* \sin \beta^*$$

$$= (0.0970)(0.19794) / (0.99528)(0.98021)$$

$$= 0.01920 / 0.97558$$

$$=0.01968$$

$$\gamma = 88^{\circ}52'$$

Since α, β both are obtuse, while γ is acute, they are not homogeneous. This rules out the possibility of their being all obtuse. To make them all acute, adjust α^*, β^* by taking supplements. It is not difficult to obtain the following:

$$\alpha^* = 95^{\circ}34'$$

$$\beta^* = 101^{\circ}25'$$

$$\gamma^* = 90^{\circ}$$

$$\cos \alpha = 0.09896$$

$$\alpha = 84^{\circ}19'$$

$$\cos \beta = 0.19888$$

$$\beta = 78^{\circ}32'$$

$$\cos \gamma = 0.01968$$

$$\gamma = 88^{\circ}52'$$

Thus all the angles α, β, γ are acute, and accordingly homogeneous. The constants a and c can now be obtained as follows:

$$a = d_{100} / \sin \beta \sin \gamma^* = 7.099 / 0.98004 = 7.244 \text{ \AA}$$

$$c = d_{100} / \sin \beta \sin \alpha^* = 18.265 / (0.98004)(0.99528) = 18.725 \text{ \AA}$$

$$b = 8.994 \text{ \AA}$$

It is apparent that $c > b > a$, which is the Balashov's second rule. From this, our temporary label $d_{100} > b > d_{100}$ is justified. Indexing the triclinic crystal of calcium l-naphthyl phosphate

- a. Determination of the axial direction on which upper levels lie

The Balashov's rules already determine the orientation of three axes a , b , c and the crystal is found to be mounted on b axis, although we are not certain of the direction of b^* . This is determined by using right-hand coordinates. Fig. 9c shows the orientation of the film with respect to the camera and x-ray. The observer is standing at the position such that the x-ray is passing through the sphere of reflection from left to right and the rotation dial is in front of the observer. In the zero level picture, the axial labels a^* , c^* and their directions are already fixed by the Balashov's rules as in Fig. 9 a. This will, in turn, fix the axial labels and their directions in Fig. 9 b and c. In Fig. 9 b, a^* c^* is assumed to lie in a horizontal plane. When c^* rotates toward a^* , from the right-hand coordinate, the positive b^* must be vertical above the plane, i.e., positive b^* is away from rotation dial. Since upper levels lie in the directions away from rotation dial, they must mount in the positive b^* direction.

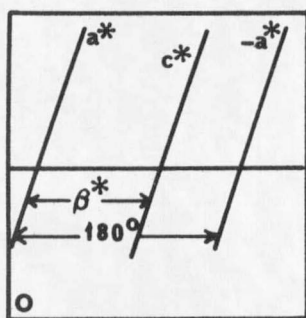
b. Calculation of the length and location of the axial projection.

In the calculation of the axial projection length, we are concerned with the relative lengths of a^* , b^* , c^* rather than the absolute lengths. For ease of calculation, the relative lengths of a^* , b^* , c^* will be used. The cell constants found are listed below.

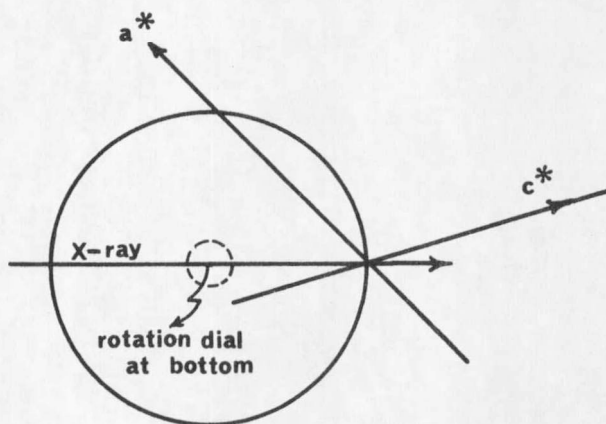
$$a=7.244\text{\AA}$$

$$b=8.994\text{\AA}$$

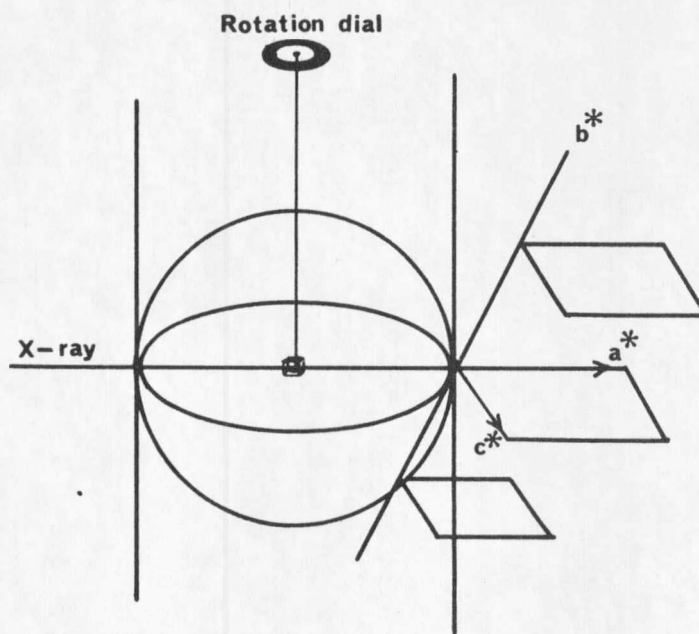
$$c=18.725\text{\AA}$$



a.



b.



c.

Figure 9 Orientation of film with respect to camera and x-ray

$$\begin{aligned} \alpha &= 84^{\circ} 19' & \beta &= 78^{\circ} 32' & \gamma &= 88^{\circ} 52' \\ d_{100} &= 7.099 \text{ \AA} & d_{010} &= 8.950 \text{ \AA} & d_{001} &= 18.265 \text{ \AA} \\ \alpha^* &= 95^{\circ} 34' & \beta^* &= 101^{\circ} 25' & \gamma^* &= 90^{\circ} \\ a^* &= \lambda/d_{100} & b^* &= \lambda/d_{010} & c^* &= \lambda/d_{001} \\ a^*:b^*:c^* &= 1/d_{100}:1/d_{010}:1/d_{001} = 1/7.099:1/8.950: \\ & & & & & 1/18.265 = 2.57:2.04:1 \end{aligned}$$

Let $a^*=2.57$ $b^*=2.04$ $c^*=1$

The b^* projection = OM

$$\begin{aligned} &= b^*(1 - \sin^2 \alpha^* \sin^2 \gamma^*)^{1/2} \\ &= 0.254 \end{aligned}$$

$$\begin{aligned} \cos p &= ((b^* \cos \alpha^*)^2 + b^{*2} (1 - \sin^2 \alpha^* \sin^2 \gamma^*) - (b^* \sin \alpha^* \cos \gamma^*)^2) / \\ & \quad 2b^* \cos \alpha^* b^* (1 - \sin^2 \alpha^* \sin^2 \gamma^*)^{1/2} \\ &= -0.97867 \end{aligned}$$

$$p = 180^{\circ} + 11^{\circ} 51' = 191^{\circ} 51' \quad \text{or} \quad 180^{\circ} - 11^{\circ} 51' = 168^{\circ} 9'$$

The former value is in the third quadrant, while the latter value is in the second quadrant. α^* and γ^* are used to determine the correct location for b^* projection as discussed previously. Since α^* and γ^* are both obtuse, the b^* projection lies in the third quadrant. Hence, $p = 191^{\circ} 51'$.

Indexing the triclinic crystal of calcium l-naphthyl phosphate:

The indexing of calcium l-naphthyl phosphate is illustrated in Fig. 10 a, b, c, d. Two things are considered below.

a. Since the γ^* angle is 90 degree, the reciprocal lattice axial line okl should appear as a straight line on each upper level.

This was found to be the case except those okl lines were too weak

to see for k being odd due to the existence of a pseudo b -glide plane. The other reciprocal lattice axial line hko was not a straight line for all upper levels.

b. For fourth level, the $h4l$ line shows up as a straight line on the film, because it happens to pass through the rotation axis.

Index-checking data:

For the checking of the indexing, I have written an IBM 1620 computer program (Fortran I). The results of the index-checking for calcium 1-naphthyl phosphate are listed in Table XXXV in appendix C. More than one thousand reflections have been checked and all gave percentage errors less than 5%. Thus, indexing is correct for this crystal. The successful solution of the structure further confirms the correct indexing of the equi-inclination photographs.

